Fragmentation of Na_3^+ clusters following He impact: Theoretical analysis of fragmentation mechanisms

D. Babikov and E. Gislason[a)]
Department of Chemistry, University of Illinois at Chicago, SES (M/C 111), 845 West Taylor Street, Chicago, Illinois 60607-7061

M. Sizun, F. Aguillon, and V. Sidis
Laboratoire des Collisions Atomiques et Moléculaires, Bât. 351, Unité Mixte de Recherche C8625, Université Paris-Sud XI, 91405 Orsay Cedex, France

(Received 28 January 2000; accepted 2 March 2000)

The process of Na_3^+ cluster ion fragmentation following excitation by a fast He atom is studied using a theoretical procedure developed earlier. The collision with He leaves Na_3^+ in any of three electronic states, and each of these can fragment into three product channels ($Na_2^+ + Na$, $Na_2 + Na^+$ and $Na + Na + Na^+$). Attention is focused on understanding both the dynamics of the Na_3^+–He interaction and the post-collisional fragmentation of the excited cluster. Four simple fragmentation mechanisms are proposed to describe the major features of the process. Contributions of these mechanisms to different fragmentation pathways are determined and their dependence on the initial internal energy of the cluster is studied. Fragmentation intensity maps are calculated and good agreement with experiment is obtained. © *2000 American Institute of Physics*. [S0021-9606(00)01620-2]

I. INTRODUCTION

The fragmentation of the sodium cluster ion Na_3^+ following collision with a He atom at 263 eV center-of-mass energy has recently been investigated experimentally.[1–3] The following processes were observed:

$$\begin{aligned} Na_3^+ + He &\rightarrow Na_2^+ + Na + He \quad \text{(channel A)} \\ &\rightarrow Na_2 + Na^+ + He \quad \text{(channel B)} \\ &\rightarrow Na + Na + Na^+ + He \quad \text{(channel C)}. \end{aligned} \tag{1}$$

The experimental results show evidence for two qualitatively different fragmentation mechanisms. The first involves an electronic excitation process, which brings the cluster to a dissociative state that rapidly fragments. The second involves an impulsive process whereby sufficient momentum is transferred from the He atom to the atoms in the cluster to induce fragmentation on the ground electronic state. However, a more detailed examination of the experimental data suggests that several simple mechanisms are involved in the fragmentation process.

We have studied process (1) theoretically.[4–6] The calculations make use of the fact that the Na_3^+–He collision is a fast process ($t_{coll} \sim 10^{-15}$ s) in comparison to the cluster vibrations ($t_{vib} \sim 10^{-13}$ s). This allows us to study the Na_3^+–He encounter separately from the fragmentation of Na_3^+, and, in addition, the collision is treated by assuming that the Na nuclei are fixed. In the encounter the He passes near or through the Na_3^+. The fragmentation of the Na_3^+ on the three electronic states after the He departs is studied using the trajectory surface hopping (TSH) approximation. Special attention is paid to the conical intersection of the two excited electronic states and to the avoided crossing in the product region between the ground and first excited state. The earlier theoretical work focused on calculating total cross sections[4] and their dependence on the initial cluster internal energy.[5] In addition, doubly differential cross sections of intensity plotted against the Na_3^+–He scattering angle and the kinetic energy of the products were calculated[4,6] and compared with the experimental results for process (1).

In the present work we seek to determine the various fragmentation mechanisms that lead to the product channels in (1). For a proper understanding of a mechanism one needs to know both how the He interacts with the various Na nuclei during the Na_3^+–He encounter and also how the Na nuclei interact with each other as the Na_3^+ fragments after the He has departed. Most of this work is done for fragmentation to channel *A* on the ground electronic state; this corresponds to the common case of electronically adiabatic dissociation on the ground state of a polyatomic molecule. We also apply our methodology to fragmentation processes that involve an excited electronic state, because we wish to know if this gives rise to additional important mechanisms. Finally, we examine how the initial internal energy of the Na_3^+ cluster affects the relative importance of the various mechanisms.

II. THEORY

The theoretical procedure is described in detail elsewhere[6] and is briefly summarized here. The three lowest singlet adiabatic potential-energy surfaces (PESs) of Na_3^+ are computed from Kuntz's DIM (diatoms in molecules) treatment of this system.[7,8] We identify the ground state as state 1, and the first and second excited states as states 2 and 3,

a)Author to whom correspondence should be addressed. Electronic mail: gislason@uic.edu.

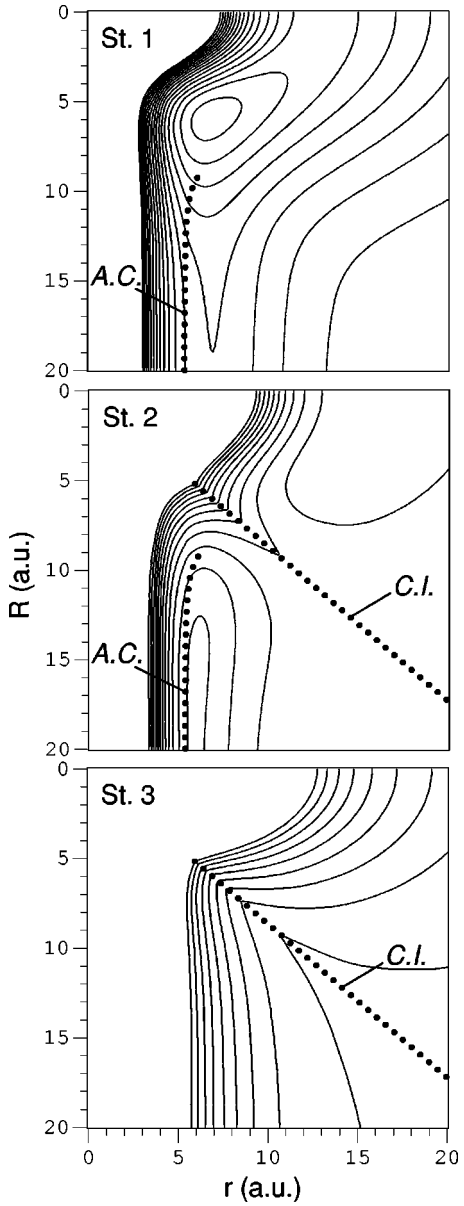

FIG. 1. Contour plots of the three PESs for T-shaped Na_3^+ as a function of Jacobi coordinates (r,R). Zero energy corresponds to completely separated atoms. Contour lines are given between -2 and 2 eV with interval of 0.25 eV. The PES of state 1 (upper view) exhibits a well of -2.12 eV in equilateral geometry. For large R, it displays a valley leading to the $Na_2^+ + Na$ products (-0.98 eV). The PES of state 2 (intermediate view) at large R has a valley, leading to the $Na_2 + Na^+$ products (-0.75 eV). State 3 (lower view) leads to the three-body fragmentation $Na + Na + Na^+$. States 1 and 2 have an avoided crossing in the product region (labeled A.C.). States 2 and 3 exhibit a conical intersection (labeled C.I.) in equilateral geometry.

respectively. States 1 and 2 have an avoided crossing in the product region and states 2 and 3 exhibit a conical intersection in the equilateral configuration (see Fig. 1). The couplings between electronic states of Na_3^+ in the presence of He are calculated in the DIM formalism, but they also include Na–He–Na three-center-interaction terms.[6] The Na_3^+ is prepared with zero rotational energy and at a fixed classical vibrational energy with random phases. Next the Na_3^+–He collision at a relative energy of 263 eV is treated using the classical path approximation[9] for the He motion with the Na nuclei frozen (the sudden approximation). The instantaneous potential energy seen by the He is calculated using the semiclassical energy conserving trajectory (SCECT) method.[10] In most cases the He interacts strongly with only one Na atom, but multiple hits do occur. After the He departs, the Na_3^+ is left with population in the three electronic states, and additional momentum has been transferred to each Na nucleus. Clusters with insufficient energy to fragment are not considered further. The final step of the calculation is a TSH study of the fragmentation of Na_3^+ with proper treatment of the conical intersection and avoided crossing.[11,12]

In the experimental work,[1–3] the Na_3^+ clusters are probably produced as the result of thermal fragmentation of larger clusters, which were previously ionized by an electron beam. After such a process Na_3^+ clusters in the ground electronic state have negligibly low (thermal) rotational energy, but significant amounts of vibrational excitation (typically up to the dissociation limit of Na_3^+). Consequently, we have performed calculations for three values of the initial vibrational energy $E_{vib} = 0.02$, 0.5, and 1 eV. The first value corresponds to the zero-point-energy of the cluster, and the last is just 0.14 eV below the dissociation limit to channel A.[6] A total of 50 000 collisions with randomly chosen initial conditions was studied. The Na_3^+–He impact parameter and the orientation of the cluster plane were chosen randomly. The calculation was stopped when two Na–Na distances exceeded 18.5 a.u. At that point the product channel and product properties were determined. In a few cases the excited cluster had not dissociated after a time of 400 000 a.u. These events were not considered further.

To better understand the fragmentation mechanisms we have also done a series of calculations for a fixed initial shape of Na_3^+. This is an elongated T-shaped cluster when the distance r between two nuclei is 6.4 a.u. and the distance R from the third atom to the center-of-mass of the other two is 11.5 a.u. This configuration corresponds to a classical turning point of Na_3^+ with 1.0 eV of vibrational energy. We have seen earlier[6] that this is a typical configuration for excitation to state 2 for a hot Na_3^+ cluster. One property monitored during these calculations was the location of the He when it passes through the plane of Na_3^+. These calculations give a useful qualitative picture of the excitation process in the Na_3^+–He collision. To distinguish the two types of atoms in this bound cluster ion, we shall refer to the two close atoms as the ''dimer'' and the distant atom as the ''monomer.'' Clearly the two atoms of the dimer are strongly bound, whereas the monomer is only weakly bound to the dimer. We also monitored which atom is ejected from the cluster when it fragments into an atom and a diatomic.

Any process induced by the Na_3^+–He collision can be assigned to a particular pathway by specifying the final product channel (A, B, or C) and the electronic state of Na_3^+ (1, 2, or 3) just after the collision with He.[4–6] Thus, collision and dissociation into two and three fragments, respectively, on the ground state correspond to pathways $A1$ and $C1$. Similarly, excitation of state 2 or 3 by He, followed by adiabatic fragmentation corresponds to pathways $B2$, $C2$, or $C3$. Finally, the ''off-diagonal'' elements ($A2$, $A3$, $B1$, and $B3$) correspond to pathways with nonadiabatic transitions during the fragmentation process. Specification of these pathways

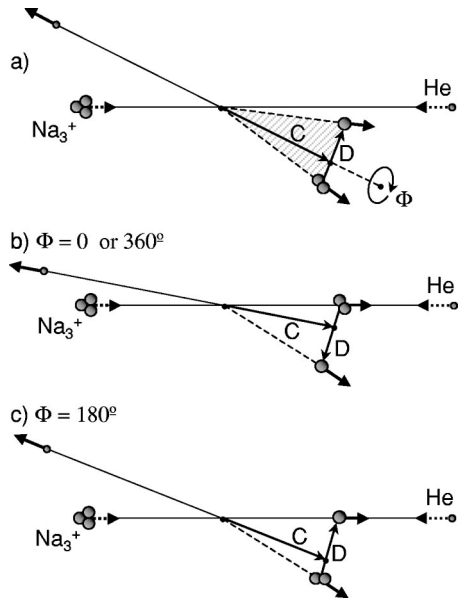

FIG. 2. Definition of Φ angle in Na_3^+ fragmentation after the collision with a He atom. The figure shows the Na_3^+–He center-of-mass reference frame. Initial velocity vectors for all species are dashed and the final velocity vectors are solid. Vector **C** locates the center-of-mass of Na_3^+ after the collision. Vector **D** connects the diatomic center-of-mass and the atomic fragment. (a) Definition of Φ angle (general situation). See text for further details. The fragmentation plane is shaded. (b) Example of the direct binary collision: $\Phi=0$ or 360°; (c) Example of the ''diatom'' process: $\Phi=180°$.

implies that there is at most one hop between surfaces during the fragmentation process. (Pathway *A*3, however, requires a minimum of two transitions as the system hops from state 3 to state 2 and then from state 2 to state 1.) In fact, multiple hops do occur but they are rare.

An important characteristic of process (1) is the time scale of the fragmentation. We denote the fragmentation time as $T_{\rm fr}$, and we define it as the time when two Na–Na distances become greater than 18.5 a.u. The zero of time is taken as the instant when the He departs the Na_3^+ fragment, and we begin the TSH calculation. Atomic units are used and for comparison typical vibrational periods for the normal modes of Na_3^+ are 10 000 a.u.

One of the most important observables in the two-body fragmentation process is the angle between the collision plane and dissociation plane, denoted Φ. This angle is routinely used to interpret experimental data.[1–3] The definitions of both planes and the angle Φ are given in Fig. 2(a). The collision plane is defined as containing the initial and final velocity vectors of the He atom. The fragmentation plane contains the final velocity vector of the He atom and the vector connecting the center-of-mass of the diatomic fragment with the atomic sodium fragment (vector **D** in Fig. 2). These two planes cross each other along the line containing the final velocity vector of He. It is obvious that the center-of-mass of the cluster (vector **C** in Fig. 2) also moves along this line after the collision. $\Phi=0°$ is defined as the case where the collision plane and the fragmentation plane coincide and the velocity of the center-of-mass of the diatomic is closer to the initial velocity vector of the He atom. This situation is shown in Fig. 2(b).

Figures 2(b) and 2(c) show two important examples of possible fragmentation processes that give products at particular Φ values. Figure 2(b) shows the collision where He collides strongly with only one atom of the cluster and ejects it from the cluster. The other two atoms are passive spectators and continue in the forward direction. In that case the collision and fragmentation planes coincide and $\Phi=0°$ or $\Phi=360°$. We shall see that these ''binary'' collisions are very important in the fragmentation process. By comparison Fig. 2(c) shows the case where the collision with He ejects two sodium atoms from the cluster. In that case the third Na atom is a passive spectator and continues in the forward direction. Again the collision plane coincides with the dissociation plane, but now $\Phi=180°$ for this ''diatom'' process. Our definition of Φ coincides with the definition of the experimental group[1–3] for product channel *A*, but for channel *B* we reverse their definitions for $\Phi=0$ and $\Phi=180°$. This difference does not cause any confusion in this paper because no experimental Φ-distributions were obtained for channel *B*.

It is also possible to define Φ for the case of three body fragmentation. The relative velocities between each pair of Na nuclei are determined, and the smallest relative velocity identifies the (pseudo) diatomic fragment. The third Na nucleus is identified as the ejected atom. The definition of Φ is then made as before.

Another important observable of the fragmentation process is ϵ, the sum of the kinetic energies of the two or three fragments in the Na_3^+-center-of-mass reference frame. This energy, as well as the angle Φ, are experimental observables. Intensity contour maps as a function of the energy spectrum of the dissociation fragments and the Φ angle have been obtained experimentally,[1–3] and we will compare our results with those data.

During the collision with He each of the Na nuclei receives a momentum transfer due to the interaction with He. It is useful to denote the three Na nuclei by *X, Y*, and *Z*, and identify the Na atom that receives the largest momentum transfer as *X*. Thus, we say that He ''hits'' atom *X*. (Of course, all three Na nuclei gain momentum from He, but it is usually the case that one receives a much larger impulse, so it is reasonable to say that He hits *X*.) If the cluster then fragments into an atom and a diatomic, there are two possibilities. In one case $X+YZ$ is produced, and in the other *X* is combined with *Y* or *Z*. We assume for definiteness in that case that the products are $XY+Z$. When the product is *XY* it is useful to define another angle ψ. We identify the vector momentum transferred to atom *X* as **p**, where **p** in general is not confined to the plane of the Na_3^+. Then ψ is defined as the angle between **p** and the vector drawn from *X* to the product atom *Z* (see below).

III. ANALYSIS OF MECHANISMS FOR PATHWAY *A*1

We have calculated total cross sections for each pathway, and the results for $E_{\rm int}=1.0$ eV are summarized in the fragmentation matrix shown in Table I. These cross sections have been discussed in details in earlier papers.[5,6] Here we note that the cross section for producing state 1 is about four

TABLE I. Fragmentation matrix.[a]

Product channel	Electronic state after $He-Na_3^+$ collision			Total values (observables)
	1	2	3	
A:	8.05	1.28	0.00	9.33
B:	0.65	0.94	0.00	1.59
C:	0.84	0.30	0.19	1.33
$A+B+C$:	9.54	2.52	0.19	12.25

[a]The columns labeled 1, 2, and 3 indicate the electronic states immediately after the Na_3^+–He collision, and the rows labeled *A*, *B*, and *C* denote the three possible product channels [see Eq. 1]. Each numerical entry is a total cross section in $Å^2$. Results are calculated for $E_{int}=1$ eV. The final column gives the cross section for each row summed over states 1, 2, and 3; this is the total product cross section for each channel. Similarly, the final row gives the cross sections for each column summed over channels *A*, *B*, and *C*; these are the total cross sections for populating states 1, 2, and 3 in the collision with He.

times larger than that for state 2, which in turn is more than ten times greater than for state 3. Pathway $A1$ is the dominant process, but most other pathways have significant cross sections. Only $A3$ and $B3$ are unimportant.

Figure 3 shows a distribution of fragmentation products plotted against the fragmentation time T_{fr} and the angle Φ for the nine pathways for $E_{int}=1.0$ eV. We consider first the $A1$ pathway, which has the largest cross section (see Table I). In addition, it is the simplest to analyze because the entire process takes place adiabatically on the ground electronic state. A number of results are immediately apparent. First, there is a high density of points (trajectories) at small times near $\Phi=0$ or 360°. We shall see that most of these events are due to a binary collision where He hits one Na atom hard and ejects it from the Na_3^+ cluster [see Fig. 2(b)]. Second, there are many points at large times, much larger than the vibrational periods of Na_3^+, and we shall see that these come from long-lived complexes. Finally, there is a secondary peak at small times near $\Phi=180°$. This corresponds to the diatom process described in the previous section [see Fig. 2(c)]. We conclude that a variety of mechanisms make significant contributions to the fragmentation of Na_3^+.

To determine and separate the various mechanisms we consider first the time dependence of all trajectories for pathway $A1$ with $E_{int}=1.0$ eV. Figure 4 gives a semilog plot of intensity versus T_{fr}. At long time we find that the plot is approximately linear, indicative of long-lived complexes that dissociate statistically. We have fit this data as shown in the figure, and we estimate that all collisions with $T_{fr}>30\,000$ a.u. correspond to long-lived complexes. This is confirmed by analysis of typical trajectories, which show that in general these trajectories correspond to rovibrational excitation just above the dissociation limit along with a complete sharing of energy among all degrees of freedom. We therefore, **define** a ''complex'' collision to be any trajectory with T_{fr} greater than 30 000 a.u. Also shown in Fig. 4 are the time

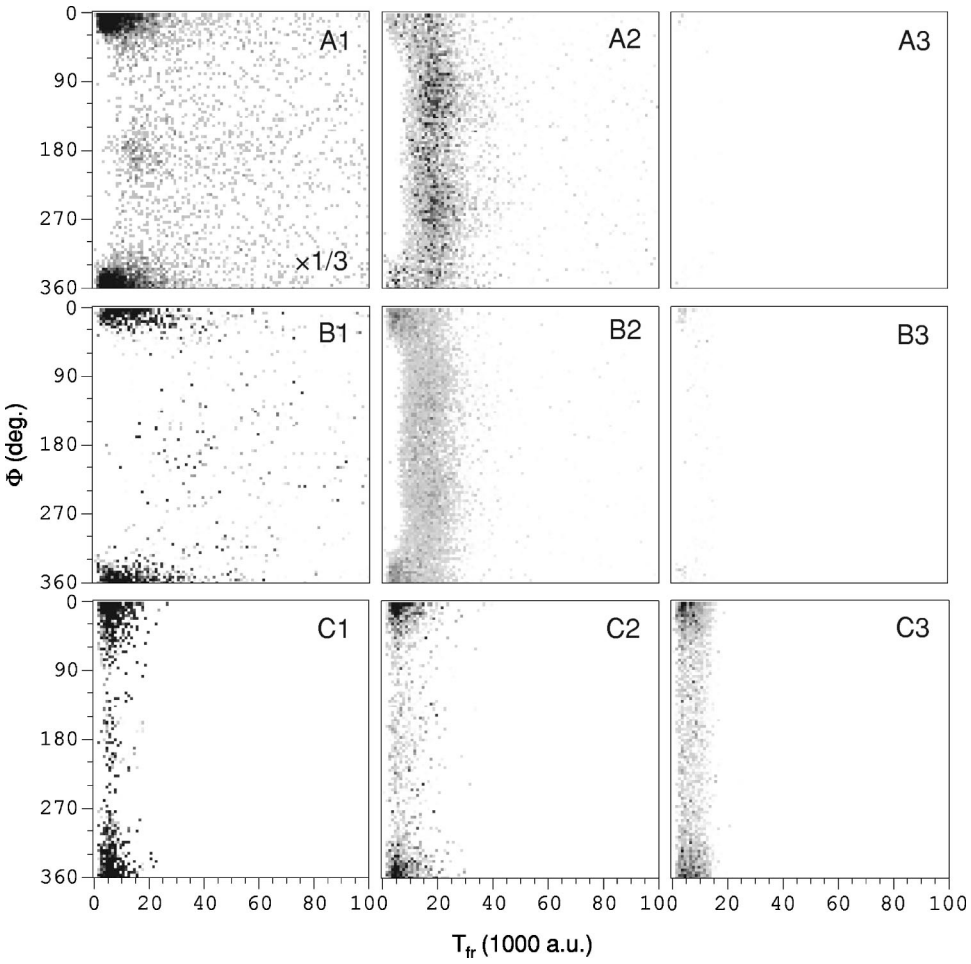

FIG. 3. Distribution of fragmentation events plotted against the fragmentation time T_{fr} and the angle Φ for all nine pathways. The labeling corresponds to the elements of the fragmentation matrix. Results were obtained for $E_{vib}=1$ eV.

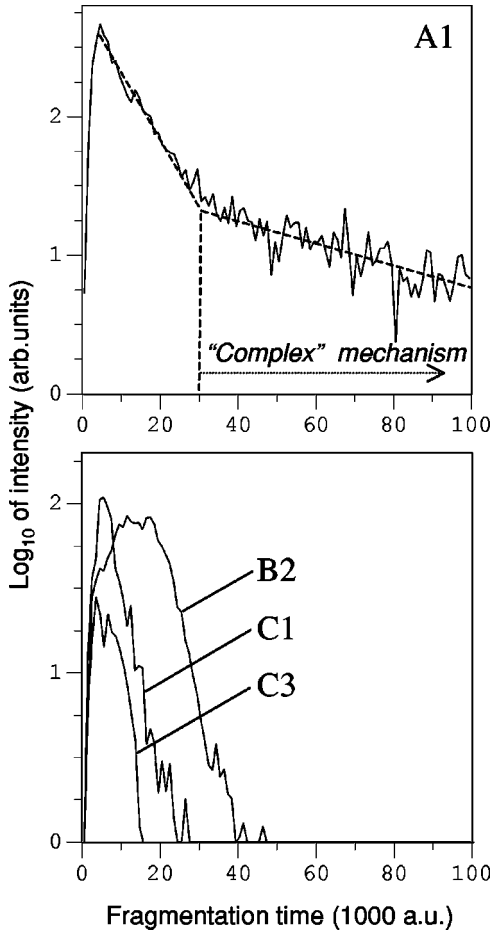

FIG. 4. Semilog plot of fragmentation intensity vs time T_{fr} for some fragmentation pathways. For the pathway $A1$ (top) a linear fit is done and the two dashed lines meet at $T' = 30\,000$ a.u.

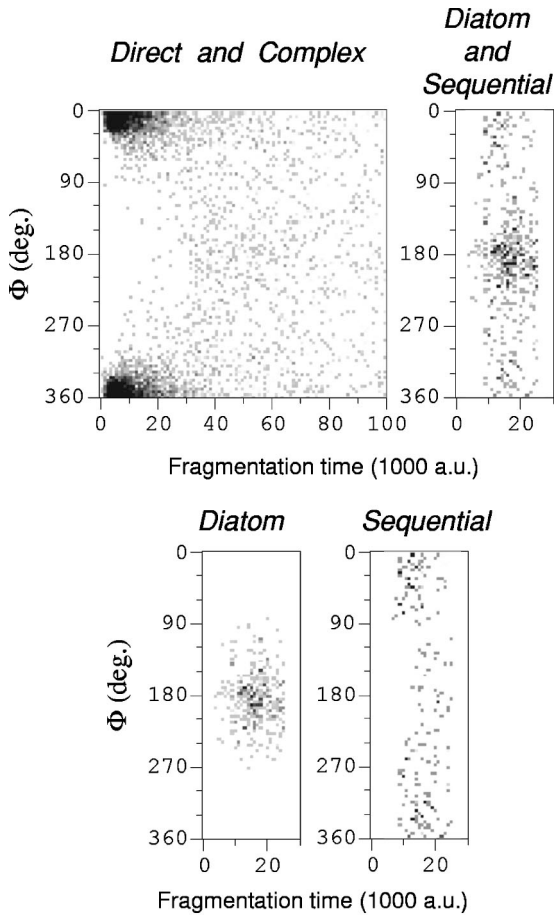

FIG. 5. Distribution of fragmentation events corresponding to different fragmentation mechanisms plotted against the fragmentation time T_{fr} and the angle Φ for $E_{vib} = 1$ eV and pathway $A1$. See text for further details.

behaviors for pathways $B2$, $C1$, and $C3$. It is clear that there are no complex trajectories in these cases (see also Fig. 3).

After we subtract the complex trajectories we next consider, from the remaining trajectories, the binary collisions. As discussed earlier we identify the three Na nuclei as *X, Y*, and *Z*, and the nuclei that receives the largest impulse from He is denoted *X*, the ''hit'' atom. We **define** ''binary'' collisions as those trajectories where the hit atom *X* is also the ejected atom, so that the diatomic product is *YZ*. In most cases we expect the products to appear near $\Phi = 0$ or 360°. The long-lived complex and binary trajectories can be separated from the others, and the results are shown in Fig. 5. As expected, the Φ-distribution of trajectories is uniform for the complex mechanism.

The trajectories that remain show intensity peaks at $\Phi = 0$, 180°, and 360° (see Fig. 5). They correspond to cases where the hit atom *X* emerges in the diatomic product *XY*. As discussed earlier there are two types of ideal collisions that lead to peaks at $\Phi = 180°$ and also at $\Phi = 0$ or 360°. The first is the case shown in Fig. 2(b), where the struck atom *X* reacts with atom *Y*, while atom *Z* remains a passive spectator and continues in the forward direction. In that case $\Phi = 180°$, and we call that a ''diatom'' reaction. The angle ψ, shown in Fig. 6, should be greater than 90° for this case to be certain that there is no *XZ* collision. The second ideal collision occurs when the struck atom *X* hits atom *Z* head on. This corresponds to $\psi = 0$. Since they have the same mass, *Z* is ejected with all of the energy, *X* slows to the same velocity as *Y*, and the *XY* molecule appears in the forward direction. In that case $\Phi = 0$ or 360°. We call this the ''sequential'' mechanism. Of course, real collisions will not be so simple, and there will be a spread in the ψ and Φ angles. Figure 6 shows a two dimensional plot of all remaining trajectories against ψ and Φ. The angle $\psi = 90°$ separates trajectories into two discrete groups.

We conclude that the angle ψ is a useful way to separate diatom and sequential trajectories. Therefore, we **define** the ''diatom'' mechanism to be all trajectories where the product is *XY* and $\psi > 90°$. In addition, we **define** the ''sequential'' mechanism to be all trajectories producing *XY* with $\psi < 90°$. The distribution of points for these two mechanisms plotted against T_{fr} and Φ are also shown in Fig. 5. We have now separated all possible trajectories into four mechanisms.

The separation scheme is summarized in Table II. We call the binary and diatom mechanisms ''direct'' because the hit Na atom *X* does not interact with one or both of the *YZ* pair (at least in the ideal case). By comparison, we call the sequential and complex mechanisms ''indirect'' because atom *X* must interact strongly with both *Y* and *Z*. Table II also gives the fraction of all trajectories that fall into the four

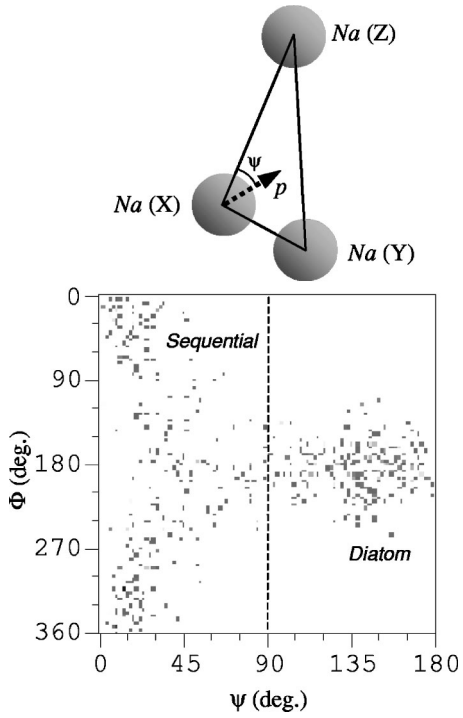

FIG. 6. Distribution of fragmentation events corresponding to the sequential and diatom mechanisms of fragmentation plotted against the angles ψ and Φ for $E_{vib}=1$ eV and pathway $A1$. The top shows the definition of the angle ψ. In the bottom part the vertical dashed line at $\psi=90°$ illustrates the last step of the separation procedure.

categories for $E_{vib}=1.0$ eV. It is not surprising that 63% of all reactions occur by the binary mechanism, because this was already apparent in Fig. 3. The binary mechanism has long been known to be very important in fragmentation processes.[13] It is somewhat more surprising to find that nearly one-third (29%) of all reactions come from long-lived complexes. Finally the diatom and sequential mechanisms make relatively small and equal contributions.

To better understand these results we have made a detailed examination of trajectories for the hot cluster, both for the fixed T-shaped Na_3^+ cluster (see Sec. II) and also for the general case. The analysis shows that the binary mechanism occurs whenever the He atom makes a direct hit (a Na–He impact parameter less than 2 a.u.) on any of the three Na nuclei. In fact, for the fixed T-shaped cluster this is the only important mechanism when the distant atom (the monomer) is hit. The calculations show that long-lived complexes are caused by softer hits on one of the Na atoms; in this case, the typical Na–He impact parameter is about 2 a.u. The sequential mechanism occurs when the He hits on the outside of the cluster and knocks one of the Na atoms directly toward a second, knocking that second atom out of the cluster. For the fixed T-shaped cluster this always involves knocking one of the atoms in the dimer towards the monomer and knocking the monomer out of the cluster. Finally, the diatom mechanism only occurs when one Na atom is far from the other two. The He passes through the inside of the cluster ion and hits one atom of the dimer. This atom recoils out of the cluster and pulls the second atom of the dimer along with it. This process occurs readily because both atoms in the dimer are only weakly bound to the monomer.

Table II also gives the contributions of the four basic fragmentation mechanisms to pathway $A1$ at the other two initial internal energies ($E_{int}=0.02$ and 0.5 eV) of the cluster. (Absolute values of corresponding total cross sections were published elsewhere.[5,6]) The direct binary mechanism dominates in all cases, especially when the cluster is cold (94% at $E_{int}=0.02$ eV). We can see that the contribution of the complex mechanism is very small when the cluster is vibrationally cold, and it increases more then 10 times when the cluster is initially hot ($E_{int}=1.0$ eV). Finally, the contribution of the sequential mechanism does not depend on internal cluster energy, while the diatom mechanism disappears completely when the cluster is cold.

We believe we can explain all of these results. The Na_3^+ cluster is fairly ''large;'' the bond length at the equilateral minimum is 6.78 a.u. By comparison, the He is small, and it must pass within 2 a.u. of an Na nucleus to give it a large impulse. Simple geometry guarantees that only rarely does a He atom collide strongly with two Na nuclei. Thus, the only way to impart considerable impulsive energy to the Na_3^+ ion is for the He to hit one nucleus very hard. In most cases that Na is ejected, giving rise to the binary mechanism. If the Na_3^+ is initially excited, a softer hit is sufficient to excite the cluster above the fragmentation limit. In addition, all of the vibrational modes of Na_3^+ are already excited, so it is much easier for the hit atom to share energy with the other two and

TABLE II. Scheme for separation of mechanisms.[a]

Fragmentation mechanisms		Separation steps and criteria			Contributions (%) to $A1$		
		Step I	Step II	Step III	ZPE	0.5 eV	1 eV
Direct	Binary	$T_{fr}<T'$	$X+YZ$		94	82	63
	Diatom	$T_{fr}<T'$	$XY+Z$	$\psi>90°$	0	1	4
Indirect	Sequential	$T_{fr}<T'$	$XY+Z$	$\psi<90°$	4	4	4
	Complex	$T_{fr}>T'$			2	13	29

[a]See text for the definitions of the fragmentation mechanisms and more complete description of the separation criteria. Step I separates trajectories corresponding to the complex mechanism of fragmentation. T_{fr} is the fragmentation time and $T'=30\,000$ a.u. Step II separates the binary mechanism from the rest of trajectories. X is the Na atom in the cluster XYZ that is hit by the He atom. Step III assigns the rest of the trajectories to either the diatom or the sequential mechanism of fragmentation. The angle ψ is shown in Fig. 6. The contributions of these mechanisms to pathway $A1$ are shown for three values of the initial internal energy of the Na_3^+ cluster. ZPE, the zero-point energy of Na_3^+, is 0.02 eV.

give rise to the complex mechanism. The sequential mechanism can occur whenever the He knocks one Na atom directly at another, so this mechanism should persist even when the cluster is cold. Finally, we have seen that the diatom mechanism can only occur when one Na atom in the cluster is weakly bound to the other two, so this mechanism vanishes for the cold cluster.

Two additional conclusions were reached from this analysis. First, whenever the diatom mechanism occurs, the He atom has passed through the interior of the Na_3^+ cluster. Similarly, if the sequential mechanism has occurred, the He has hit the Na_3^+ on the outside of the cluster.

IV. OTHERS PATHWAYS OF FRAGMENTATION

The previous section describes how impulsive energy transfer from He to one Na nucleus followed possibly by additional Na–Na collisions determines the fragmentation mechanisms for pathway $A1$. When the cluster is hot the major conclusions are that the binary mechanism dominates, that complex formation is also important, and that both the diatom and sequential mechanisms, which involve secondary Na–Na collisions, make small but significant contributions. The fragmentation intensity for $A1$ plotted against Φ and T_{fr} in Figs. 3 and 5 foretold most of these conclusions. Peaks due to the binary mechanism are seen at short time near $\Phi = 0$ and 360°. By comparison, complex trajectories appear at large time with a uniform Φ distribution. Finally, the diatom mechanism gives a broad peak at relatively short time near $\Phi = 180°$.

We wish to apply the mechanisms developed for pathway $A1$ to other pathways to see what light they can shed on those fragmentation processes. There are two quite different types of pathways to consider. First, there are those ($B1$ and $C1$) that originate in the ground electronic state. (Recall that we can apply the mechanisms developed for two body dissociation to three body fragmentation such as $C1$ by following the procedure described in the theory section.) These are discussed below, and we shall see that the four mechanisms are very useful for understanding these pathways.

The other type of pathway is one that originates in an excited electronic state. In that case repulsive energy release along one or more of the Na_3^+ coordinates also contributes to and may dominate the fragmentation process. The mechanisms developed in the previous section and summarized in Table II uniquely separate all possible fragmentation trajectories into four groups. Consequently, the procedure can be applied to dissociation in an excited electronic state. However, it is not clear what can be learned in this case. Experimentalists[1–3] show that a certain fraction of collisions with He gives fragmentation in excited electronic states with very little impulsion given to the three Na nuclei of the cluster ion. In this case the fragmentation is determined by the repulsive PESs of the excited states, and it is irrelevant which of three Na nuclei receives the strongest hit from the He atom. We call this limiting case the pure ''electronic'' mechanism. An application of our separation procedure summarized in Table II shows that in this limit there will be no complex formation and the percentages for the binary, diatom and sequential mechanisms will all be equal. In addition, the fragmentation intensity plotted against Φ and T_{fr} in the fashion of Fig. 3 will show a vertical band restricted to small fragmentation times and with a uniform Φ distribution. We shall see that the results for pathways $B2$ and $A2$ are close to this limit when the cluster is hot. Nevertheless, we shall also find for these pathways as well as for $C2$ and $C3$ that certain of the mechanisms developed for $A1$ continue to play a role in fragmentations that originate in excited electronic states.

TABLE III. Fragmentation mechanism contributions to other pathways.[a]

Fragmentation mechanisms	E_{int}	Contribution (%) to different fragmentation pathways					
		$B1$	$C1$	$A2$	$B2$	$C2$	$C3$
Binary	*a*	39	64	85	91	79	73
	b	83	73	51	68	73	77
	c	78	78	28	43	75	63
Diatom	*a*	0	7	15	9	17	23
	b	0	6	36	26	22	18
	c	3	5	34	35	15	25
Sequential	*a*	32	29	0	0	5	4
	b	2	21	9	6	6	5
	c	2	17	28	22	10	12
Complex	*a*	29	0	0	0	0	0
	b	15	0	4	0	0	0
	c	17	0	10	0	0	0

[a]Results for $E_{int} = 0.02$, 0.5, and 1.0 eV are identified by (*a*), (*b*), and (*c*), respectively.

The distributions of fragmentation products for different pathways are shown in Fig. 3 for $E_{int} = 1.0$ eV. Several mechanistic conclusions can be reached from these data. First, we see that the binary mechanism dominates in most pathways (the exception is $A2$). Second, complex formation is possible only in those pathways that involve the stable ground electronic state ($A1$, $B1$, and $A2$). Third, complete fragmentation ($C1$, $C2$, and $C3$) is always a fast process and is very fast in state 3. Fourth, pathways $A2$ and $B2$ exhibit a slight concentration of trajectories near $\Phi = 90°$ and 270°.

We now consider pathway $B1$ in detail. This requires a hop from the ground to the first excited electronic state. An examination of Fig. 3 shows that the binary and complex mechanisms are quite important, and the diatom mechanism is relatively less important than for $A1$. The various percentages for all four mechanisms at three values of E_{int} are summarized in Table III. Overall, the relative importance of each mechanism is similar to that for $A1$ for $E_{int} = 0.5$ and 1.0 eV (see Table II). Examination of trajectories for the fixed T-shaped Na_3^+ (see Sec. III) shows that for a hot cluster $B1$ comes predominantly from He hitting one of the atoms in the dimer, knocking it out of the cluster, and leaving behind a diatomic product with large vibrational energy. It is remarkable, however, to see that the fraction of binary collisions drops to 39% for cold Na_3^+; in fact, we see in Table III that the binary mechanism is only slightly more effective in this case than sequential or complex. To understand this result we recall that state 1 dissociates adiabatically to $Na_2^+ + Na$ (channel *A*). To produce channel *B* ($Na_2 + Na^+$) the intermediate diatomic product Na_2^+ must be produced with at least 0.27 eV vibrational energy, so it can reach the avoided crossing to form Na_2. This is very unlikely if the Na_3^+ is originally

cold.[5,6] In a ''pure'' binary collision, the ejected Na atom would not interact in any way with the remaining Na_2 dimer as it left the cluster. In that case the Na_2 dimer would have zero vibrational energy, so the fraction of binary collisions giving pathway $B1$ would be zero for cold clusters. The reality is that the departing Na^+ ion does interact with the Na_2 dimer to some extent, giving to it some vibrational energy, and a small fraction of binary collisions will lead to pathway $B1$ even for a cold cluster. Nevertheless, the binary mechanism is not an efficient way to give vibrational energy to the diatomic product when the cluster is cold. By comparison, the sequential mechanism is an efficient way to put vibrational energy into the diatomic product.

Pathway $C1$ results from three-body fragmentation in the ground electronic state. Figures 3 and 4 show that that fragmentation is fast (there are no complex trajectories) and is dominated by binary collisions with some evidence that the diatom mechanism contributes. Table III shows the sequential mechanism is also quite important. An examination of the calculations for the fixed T-shaped cluster shows that for both binary and sequential mechanisms pathway $C1$ primarily occurs when the He atom hits one of the atoms in the dimer species, thereby breaking the shortest (and strongest) bond in the Na_3^+ cluster.

We next consider the pathways that originate in state 2. In the T-shaped configuration this excited state's PES is bound along the dimer bond r but repulsive along the dimer-monomer coordinate R.[5,6] Pathway $B2$ is produced when state 2 dissociates adiabatically to Na_2+Na^+. Examination of Fig. 3 shows that there is a quite uniform band of intensity as a function of Φ except near $\Phi=0$ and 360° where binary collisions accumulate and near $\Phi=90°$ and 270°. There are some trajectories with fragmentation times larger than 30 000 a.u., but Fig. 4 shows that these do not arise from complex collisions. Table III shows that the percentages for the other three mechanisms are nearly the same when $E_{\text{int}}=1.0$ eV. This coupled with the behavior in Fig. 3 suggests that the system is nearly in the limit where the fragmentation is determined solely by the repulsion in the excited state. This occurs partly because state 2 is produced primarily when the He passes between two Na nuclei, and no nucleus receives a large impulse. Nevertheless, binary collisions are clearly favored over the diatom and sequential mechanisms, so the impulse given to Na_3^+ by He still plays a role in the fragmentation. An examination of the calculations for the fixed T-shaped Na_3^+ for pathway $B2$ shows that the monomer is ejected in 96% of the trajectories. This is not surprising, given that the PES is bonding for the dimer but repulsive along the dimer–monomer coordinate. The calculations also show that state 2 is excited most often when the He passes through the interior of the Na_3^+ cluster; this explains why the diatom mechanism is more important than the sequential. Finally, the calculations explain the intensity increases in Fig. 3 near $\Phi=90°$ and 270°. These trajectories come from collisions where He passes through the axis of the dimer just on the outside of one of the dimer atoms and then the monomer atom is ejected. In this case the collision plane contains the two Na nuclei in the dimer, whereas the fragmentation plane contains the monomer atom and is perpendicular to the plane of the Na_3^+ ion. These two planes are perpendicular to each other, and this corresponds to $\Phi=90°$ and 270°. Of course, this is the description of an ideal collision, and in general the two planes will not be always perpendicular, so there will be a range of Φ values near 90° and 270°.

We now consider the other pathways that arise from state 2. Almost all intermediate Na_2 molecules produced in state 2 have enough vibrational energy to reach the avoided crossing (more then 0.04 eV) and make the transition to the ground electronic state and form the pathway $A2$.[5,6] Thus it is not surprising that the results in Fig. 3 and the percentage of the various mechanisms are so similar for pathways $B2$ and $A2$. However, it is interesting that a small fraction of the fragmentation in pathway $A2$ for hot Na_3^+ clusters involve the complex mechanism. Presumably this occurs because the transition to the ground state at the avoided crossing puts additional vibrational energy into the Na_3^+ cluster, increasing the chance of forming a long lived intermediate complex. The results for three body fragmentation in pathway $C2$ are also similar to those for $B2$. Inspection of the calculations for the fixed T-shaped Na_3^+ shows, however, that in this case the He atom always hits one of the nuclei in the dimer hard, thereby breaking the shortest (and strongest) bond in the cluster.

Excitation of state 3 is very unlikely. For this state the PES is strongly repulsive along all three Na–Na pairs, so $C3$ is the most important pathway. Figures 3 and 4 show that fragmentation is very fast. The mechanistic results, shown in Table III, are similar to those for pathways $B2$. Thus, the binary mechanism dominates, and the diatom mechanism is

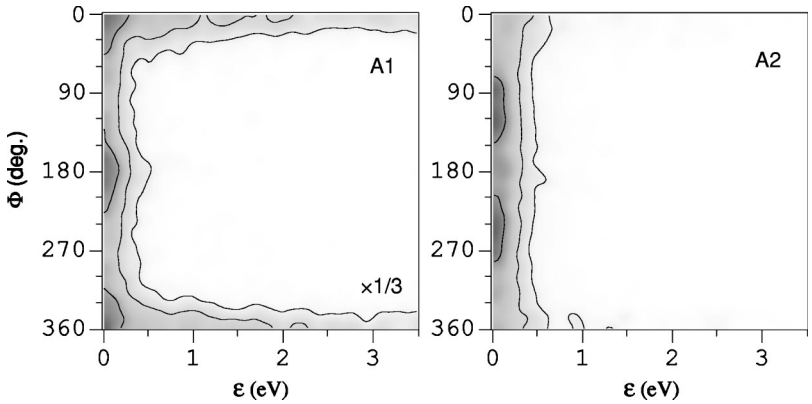

FIG. 7. Theoretical intensity contour maps plotted against the angle Φ and the relative kinetic energy of fragments ϵ for pathways $A1$ and $A2$ obtained for $E_{\text{vib}}=1$ eV.

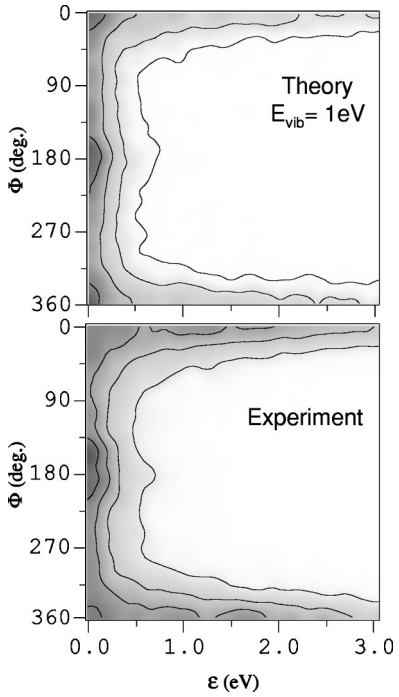

FIG. 8. A comparison of theoretical and experimental intensity contour maps plotted against Φ and ϵ for product channel A. The theoretical results were obtained for $E_{vib}=1$ eV by summing the results for $A1$ and $A2$ shown in Fig. 7.

more important than sequential. For the fixed T-shaped cluster we find that excitation only occurs when the He hits near one of the atoms in the dimer. In all cases the atom ejected with the fastest velocity comes from the dimer.

V. COMPARISON WITH EXPERIMENT

Figure 7 shows theoretical intensity contour maps plotted against the angle Φ and the relative kinetic energy of fragments ϵ for pathways $A1$ and $A2$ for $E_{int}=1.0$ eV. For $A1$ the peaks near $\Phi=0$ and 360° are due to binary collisions that can lead to large values of ϵ. The other peak near $\Phi=180°$ is due to collisions which follow the diatom mechanism. The results for $A2$ do not show the large ϵ values seen for $A1$, because excitation of state 2 does not require a hard collision of He with an Na nucleus. The peaks near $\Phi=90°$ and 270° appear prominently in the Figure.

Figure 8 shows a comparison of theoretical and experimental[1–3] intensity contour maps plotted against Φ and ϵ for product channel A (doubly differential experimental data for other pathways are not available). The theoretical results were obtained by adding together the results for pathways $A1$ and $A2$ shown in Fig. 7. (The cross section for $A3$ is negligible.) Overall, the agreement is very good. It requires the superposition of the impulsive and electronic processes, $A1$ and $A2$, respectively, to give the proper shape to the contour map. The experimentalists interpreted their results by introducing three different mechanisms for cluster fragmentation.[2] These are $IM1$, one step impulsive mechanism; $IM2$, two step impulsive; and EM, electronic mechanism. For product channel A they estimated that $IM1$ contributes 56%, $IM2$ adds 34%, and EM gives 10%. We can roughly associate their $IM1$ with our binary collisions in pathway $A1$, $IM2$ with diatom, sequential and complex collisions in $A1$; and EM with all trajectories in $A2$. Our theoretical numbers to compare with theirs are 54%, 32%, and 14%. Again the comparison is very good.

VI. SUMMARY

This article reports a theoretical study of the fragmentation of an Na_3^+ cluster ion following a collision with a fast He atom. Trajectory results are presented in the form of correlations between the time of fragmentation T_{fr} and the angle Φ between the planes of collision and fragmentation. Such a representation makes clear that very different mechanisms contribute to the fragmentation process even in the simplest pathway when the cluster always stays in the ground electronic state and fragments adiabatically. The results are explained in terms of four simple fragmentation mechanisms, representing possible scenarios of the Na_3^+–He collision and motion of the Na nuclei during the ensuing fragmentation of the Na_3^+ cluster. These are the binary, diatom, sequential, and complex mechanisms. A way to separate these fragmentation mechanisms is demonstrated, and their contributions are calculated.

The dependence of the four fragmentation mechanisms on the initial internal energy of the Na_3^+ cluster is also studied. We found that complex formation as well as the diatom mechanism of fragmentation are not efficient when the cluster is cold. This result gives an interesting prediction for future experimental studies of vibrationally cold clusters.

Finally we have applied our methodology to the analysis of other fragmentation pathways that involve an electronic excitation of the Na_3^+ cluster by the He atom and/or electronic transitions in the excited Na_3^+ while it fragments. We found that our four mechanisms of fragmentation are still useful in this case. They provide deep insight into the fragmentation process.

ACKNOWLEDGMENTS

We would like to thank J. A. Fayeton, M. Barat, and Y. J. Picard at LCAM (Orsay) for providing their experimental data and for helpful discussions.

[1] M. Barat, J. C. Brenot, H. Dunet, and J. A. Fayeton, Z. Phys. D: At., Mol. Clusters **40**, 323 (1997).
[2] M. Barat, J. C. Brenot, H. Dunet, J. A. Fayeton, and Y. J. Picard, J. Chem. Phys. **110**, 10758 (1999).
[3] M. Barat, J. C. Brenot, H. Dunet, J. A. Fayeton, Y. J. Picard, D. Babikov, and M. Sizun, Chem. Phys. Lett. **306**, 233 (1999).
[4] D. Babikov, M. Sizun, F. Aguillon, and V. Sidis, Chem. Phys. Lett. **306**, 226 (1999).
[5] D. Babikov, E. A. Gislason, M. Sizun, F. Aguillon, and V. Sidis, Chem. Phys. Lett. **316**, 129 (2000).
[6] D. Babikov, E. A. Gislason, M. Sizun, F. Aguillon, and V. Sidis, J. Chem. Phys. **112**, 7032 (2000).
[7] P. J. Kuntz, in *Atom–Molecule Collision Theory*, edited by R. B. Bernstein (Plenum, New York, 1979), p. 79.
[8] P. J. Kuntz, Mol. Phys. **88**, 693 (1996).
[9] E. Gislason, G. Parlant, and M. Sizun, in *Advances in Chemical Physics Series, State-Selected and State-to-State Ion-Molecule Reaction Dynam-*

ics, Part 2: Theory, edited by Michael Baer and C. Y. Ng (Wiley, New York, 1992), p. 321.
[10] A. E. DePristo, J. Chem. Phys. **78**, 1237 (1983).
[11] G. Parlant and E. A. Gislason, J. Chem. Phys. **91**, 4416 (1989).
[12] M. Sizun, J. B. Song, and E. A. Gislason, J. Chem. Phys. **109**, 4815 (1998).
[13] J. C. Brenot, H. Dunet, J. A. Fayeton, M. Barat, and M. Winter, Phys. Rev. Lett. **77**, 1246 (1996).